International Journal of Pharmaceutical Research and Applications
Volume 8, Issue 6 Nov-Dec 2023, pp: 753-759 www.ijprajournal.com ISSN: 2249-7781

Synthesis and Characterization of Nano Sheet-shaped Bismuth Citrate Nanocrystals

Zhifu Wu[1*] and Liyun Hu[2]
1. School of Pharmacy, Guilin Medical University, Guilin 541199, China
2. Library of Guilin Medical University, Guilin 541199, China

Submitted:20-11-2023 Accepted: 30-11-2023

ABSTRACT: Nano Sheet-shaped bismuth citrate was synthesized by hydrothermal method using bismuth nitrate, sodium hydroxide, and citric acid as raw materials.
Aims: To analyze the molecular structure and crystal morphology of bismuth citrate.
Methodology: The product was characterized using Fourier transform infrared spectroscopy, thermogravimetry, X-ray diffraction. And its surface morphology was observed by scanning electron microscopy.
Results: The crystal morphology showed the aggregation made of sheet-shaped crystal fragments.
Scientific Novelty: The molecular structures of bismuth citrate is metal ion Bi (Ⅲ) combined with acid by bidentate coordination.
Conclusion: Bismuth citrate synthesized by hydrothermal method has the advantages of high yield and stable structure compared with other traditional techniques.
Key Words: Sheet-shaped Nanocrystals; Bismuth citrate; Hydrothermal synthesis; X-ray diffraction

I. INTRODUCTION

Bismuth citrate not only has antibacterial, anti-ulcer and anti-tumor effects, but also can be used as a rocket propellant in missiles[1-4]. Bismuth citrate complexes usually exist in the form of two-dimensional layered polymers or three-dimensional reticular frameworks. In the treatment of peptic ulcer, these drugs can not only strengthen the barrier of gastric mucosa, reduce the erosion of gastric acid on peptic ulcer, but also kill Helicobacter pylori [5,6]. Ranitidine bismuth citrate (RBC) is a new drug against ulcer disease in recent years. This drug not only has the anti-gastric acid effect of H_2 receptor antagonist, but also has the effect of bismuth on protecting gastric mucosa and inhibiting pepsin activity[7]. It also has an effect on patients who are ineffective in H_2 receptor antagonists, and has a stronger bactericidal effect and a lower blood bismuth concentration, which greatly reduces the possibility of neurotoxicity due to high concentrations of bismuth. It has become a major research hotspot[8]. In this experiment, bismuth citrate was tested by infrared analysis, thermogravimetric analysis, X-ray diffraction and scanning electron microscopy. The structure of bismuth citrate was tested by infrared analysis and thermogravimetric analysis. The atomic distribution of bismuth citrate crystal was studied by X-ray diffraction. The surface morphology of bismuth citrate was observed by scanning electron microscopy.At present, the X-ray diffraction PDF pattern and related diffraction data of bismuth citrate structure have not been seen. In this paper, its structure is characterized and its crystal map is provided.

II. MATERIALS AND METHODS

Experimental instruments and test conditions

Infrared analysis was performed on an EXUS 870 Fourier transform infrared spectrometer (NICOLET, USA). The test range was 4000 cm^{-1}~ 400 cm^{-1}, the number of scans was 32 times, and the spectral resolution was 4 cm^{-1}. The phase test was performed on an intelligent high power Smart lab 2006 X-ray diffractometer (Rigaku Co., Ltd., Japan). The test voltage was 30 kV. The accelerating voltage was 5 kV. The current was 20 mA. The scanning mode was continuous scanning. The scanning speed was 4^o / min. The scanning range was 0°~ 90 ^oC . The X-ray source uses copper target Cu K_α radiation (λ= 1.54184 Å). Thermogravimetric analysis was carried out by STA 449F5 (Germany NETZSCH) instrument. The sample was 3.41mg. The test temperature is 30^oC ~ 800^oC. The heating rate is 10K/min in N_2 atmosphere. SU-5000 field emission scanning electron microscope (Hitachi, Japan), electronic balance (JA5003N, Shanghai Precision Scientific Instrument Co., Ltd.), ceramic mortar, 100 mL beaker, Buchner funnel and oven.

Experimental materials

Citric acid ($C_6H_8O_7$, AR, Tianjin Guangfu Chemical Reagent Co., Ltd.), bismuth nitrate ($Bi(NO_3)_3 \cdot 5H_2O$, AR, Shanghai Sinopharm

International Journal of Pharmaceutical Research and Applications
Volume 8, Issue 6 Nov-Dec 2023, pp: 753-759 www.ijprajournal.com ISSN: 2249-7781

Chemical Reagent Co., Ltd.), absolute ethanol (C_2H_5OH, AR, Cologne Chemical Reagent Co., Ltd.), sodium hydroxide (NaOH, AR, Shanghai Sinopharm Chemical Reagent Co., Ltd.), distilled water.

Took 10g of citric acid and dissolved it in 40ml of distilled water into a certain concentration of citric acid solution. In addition, 20g of bismuth nitrate and 6g of sodium hydroxide were weighed and dissolved in 20ml of water to form precipitation. The resulting precipitate is added to the citric acid solution, constantly stirring, dissolved and transferred to the reactor, the reactor is put into the oven, heated to 80 constant temperature reaction for 5 hours, cooled to room temperature, to get the white precipitate. Then the precipitate was filtered and washed with distilled water and absolute ethanol, and then dried in an oven to produce the white powdered product —bismuth citrate.

III. RESULTS AND ANALYSIS

Infrared spectrum analysis

Figure1 is the infrared spectrum of the synthesized product, which can be seen from

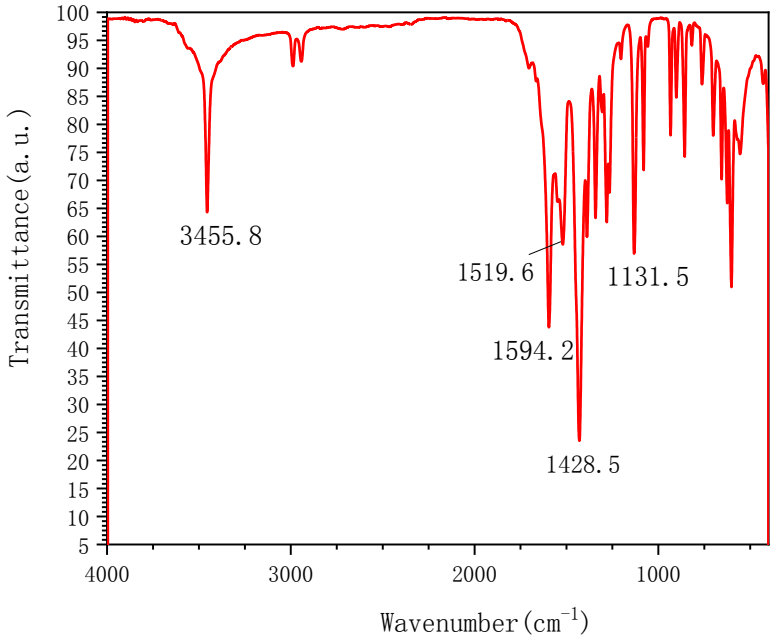

Figure 1 FTIR spectrum of synthesized product

from it that the C = O double-peak characteristic stretching vibrations of the -COO- bond are 1594.2 cm^{-1} and 1518.1cm^{-1}. Compared with the C=O bimodal characteristics of -COO- in citric acid reported in[9], it shifted from 1752.84 and 1696.88 cm^{-1} to 1594.2 and 1518.1 cm^{-1}. At the same time, the characteristic bands of COOH in the infrared spectrogram, which range from 2500cm^{-1} to 3000cm^{-1} has disappeared as a group of weak bands. There are three coordination modes between -COO- and metal ions in citric acid. They are monodentate coordination, bidentate coordination and bridge coordination. It can be judged according to the difference Δ between the symmetric vibration and the asymmetric vibration of -COO-. When Δ< 196cm^{-1} is a double tooth coordination and Δ> 196cm^{-1} is a single tooth coordination. It can be seen from Figure 2 that the Δ value of bismuth citrate is greater than the free carboxylate value of 196 cm^{-1}. It can be judged that -COO- in citric acid binds to Bi^{3+} in a bidentate manner [10].

International Journal of Pharmaceutical Research and Applications
Volume 8, Issue 6 Nov-Dec 2023, pp: 753-759 www.ijprajournal.com ISSN: 2249-7781

Thermo gravimetric analysis of bismuth citrate

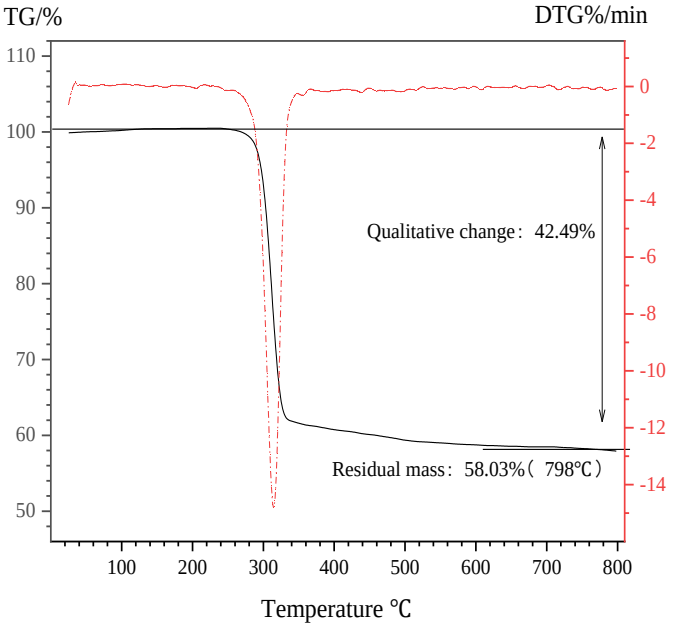

Figure 2 Thermogravimetric diagram of synthesized product

The STA 449F5 (NETZSCH, Germany) instrument was used for analysis, and the thermogravimetric analysis of the obtained product is shown in Figure 2. It can be seen from the figure that in the first stage of thermal decomposition of bismuth citrate, T1 is 25 ~ 100 °C. When heated by a thermal balance, as the temperature increases, the gas density around the bismuth citrate sample begins to change. The heavier gas continues to sink to form an airflow, which impacts the sample support assembly downwards to produce apparent weight gain assemblies. The lighter gas rises to form another airflow, which impacts the sample support assembly upwards, resulting in apparent weight loss phenomenon. In the 25 ~ 100 °C stage, the gas is mainly sinking airflow, resulting in apparent weight gain. The weight gain rate gradually increased. Then began to decrease, a slight weight gain occurred. In the second stage T2, which was 100-248℃, the thermal decomposition rate of bismuth citrate remains basically unchanged. In this range, bismuth citrate basically does not undergo thermal decomposition. However, a small amount of depolymerization or recombination may occur inside the sample near 248°C. In the third stage T3, which was 248 ~ 348°C, bismuth citrate began to pyrolyze rapidly. The sample lost a large amount of weight, and the initial decomposition temperature was 248℃. And some studies believe that bismuth citrate samples will produce carboxyl groups during thermal decomposition and then generate new carbonyl compounds-ketones. In the fourth stage T4, between 348°C and 800 °C, the residual carbon of bismuth citrate began to decompose slowly at high temperature, and finally ash was formed. Therefore, in this stage, the thermogravimetric curve changes slowly.

It can be seen from Figure 2 that when the thermogravimetric analysis of bismuth citrate was carried out at a temperature of 25 ~ 800°C, bismuth citrate lost continuously with the increase of temperature, and the mass changed by 42.49 %. The residual mass was 58.03 % at 798 °C. The final decomposition product was analyzed by infrared analysis and X-ray diffraction. The analysis showed that the final decomposition product was Bi_2O_3 and did not contain carbon material. Therefore, the content of Bi could be calculated : Bi % = 58.03 % × 208.98 × 2 / (08.98 × 2 + 15.999 × 3) = 52.05 %. The content of bismuth in bismuth citrate quality standard is 51.5 % ~ 52.5 %, and the content of bismuth in bismuth citrate meets the standard.

International Journal of Pharmaceutical Research and Applications
Volume 8, Issue 6 Nov-Dec 2023, pp: 753-759 www.ijprajournal.com ISSN: 2249-7781

X-ray diffraction analysis

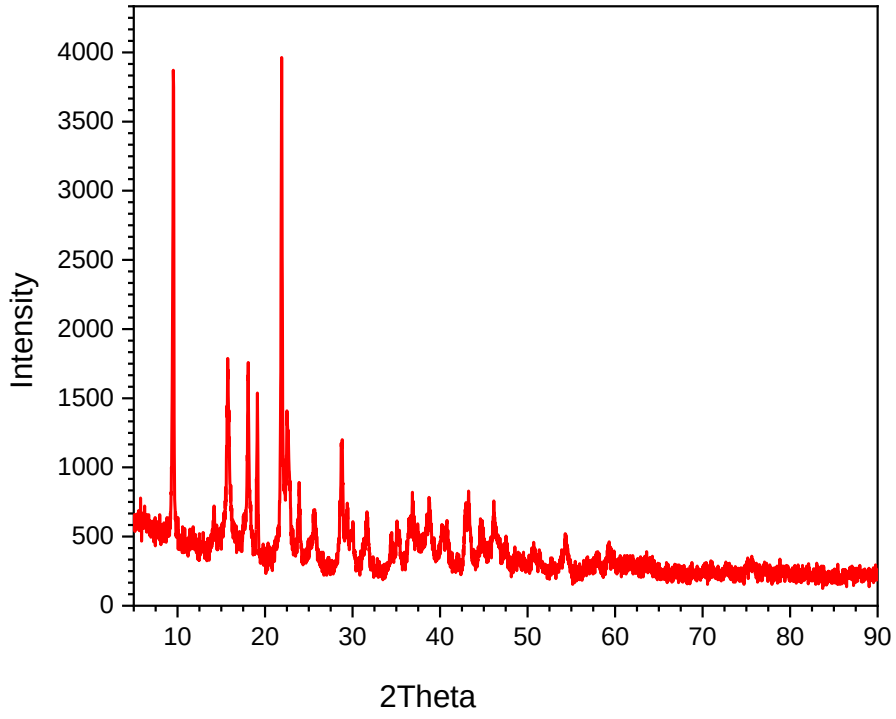

Figure 3 XRD pattern of the product

Figure 3 is the X-ray diffraction pattern of the synthesized product. It can be seen from the figure that the sample bismuth citrate has obvious diffraction peaks at 2θ of 15.78°, 18.15°, 19.15°, 21.89°, 22.53°, 24.04°, 28.93°, 36.83°, 43.36°, and 46.15°. By comparing the XRD patterns of the product bismuth citrate and the citric acid(PDF # 16-1157), it can be seen that the characteristic peak of the raw material citric acid at 2θ does not coincide with the characteristic peak of the product bismuth citrate, but shifts, indicating that citric acid reacts with bismuth nitrate to produce a new substance, which is not a simple phase superposition.

Analysis of surface microstructure

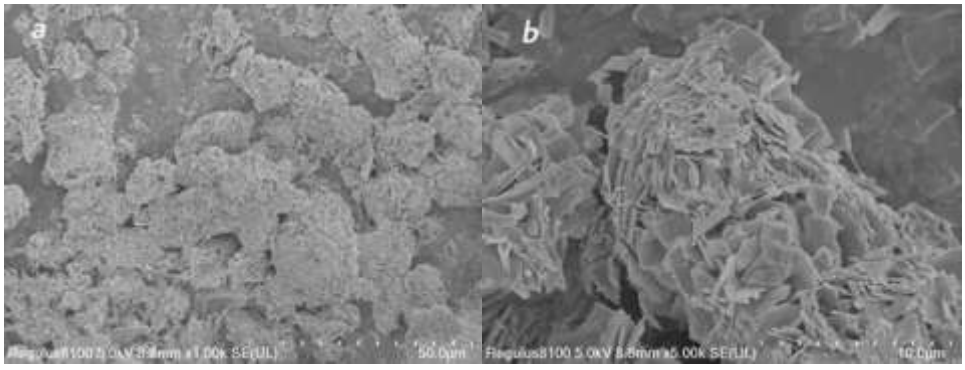

International Journal of Pharmaceutical Research and Applications
Volume 8, Issue 6 Nov-Dec 2023, pp: 753-759 www.ijprajournal.com ISSN: 2249-7781

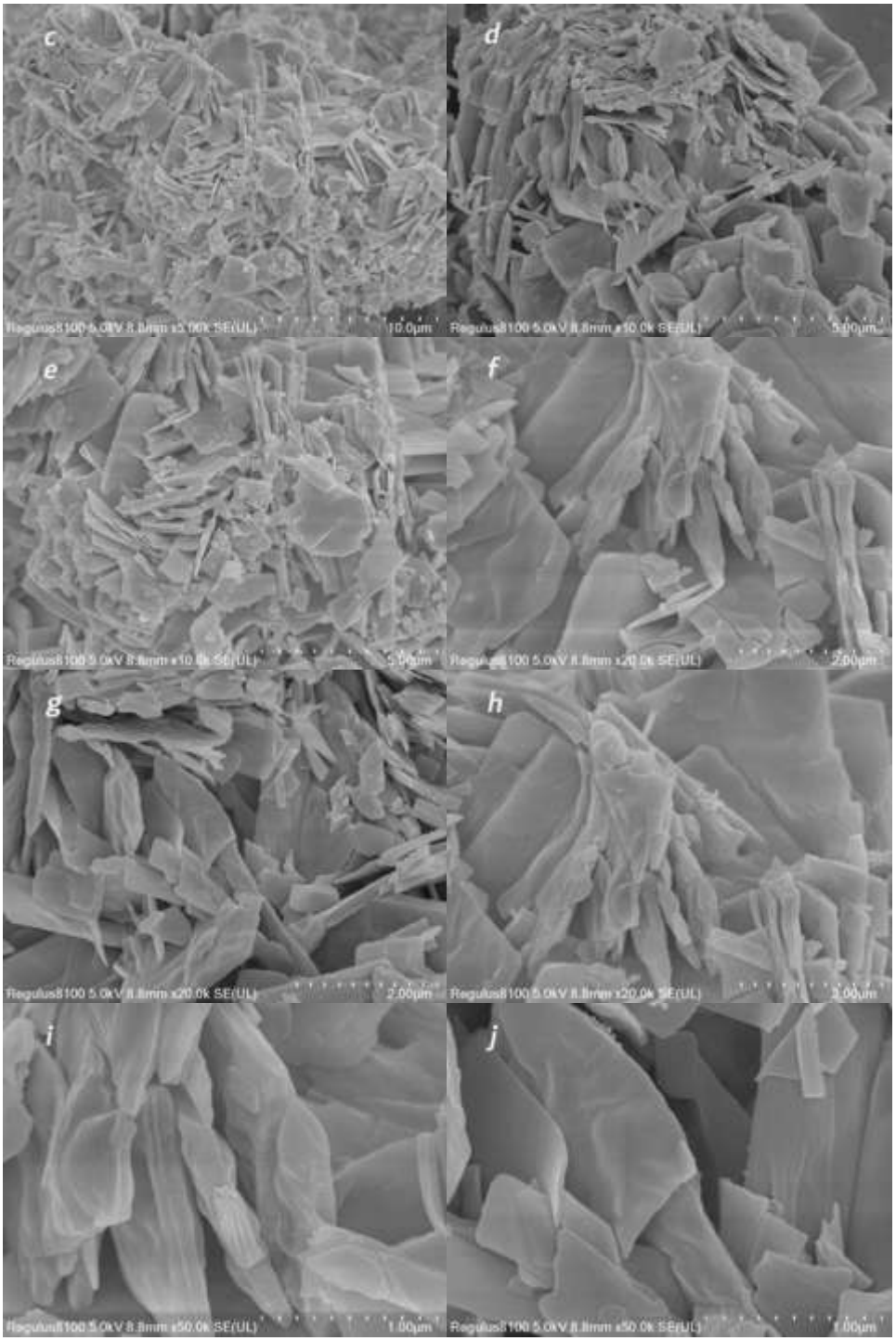

International Journal of Pharmaceutical Research and Applications
Volume 8, Issue 6 Nov-Dec 2023, pp: 753-759 www.ijprajournal.com ISSN: 2249-7781

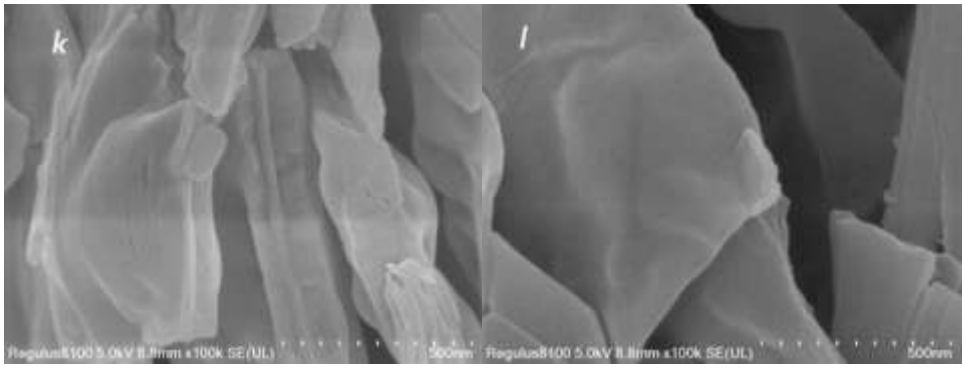

Figure 4 SEM images of the product

Magnification times：(a: 1000, b: 5000, c: 10000, d: 20000, e: 10000, f: 20000 , g: 20000, h: 20000, i: 50000, j: 50000, k: 100000 , l: 100000)

The SEM images of the product is shown in Figure 4. It can be seen from Figure 4 (a, b) that the bismuth citrate crystal is composed of flower-like particles, and the surface is not smooth. Figure 4 (c, d, e) can be seen that the flower-like particles are formed by irregular flake crystals stacked together. The surface of the wafer is smooth and the edge of the fracture is not regular. Figure 4 (f, g, h) is a 20000 times magnification of the electron microscope image. From the diagram, it can be seen that there are gaps between the stacked wafers. The fragments are not completely in contact with each other, and some fragments have cracks on the surface. In Figure 4 g, the fragments inside the flocks mostly exist in a vertical manner, while the fragments on the surface exist in a horizontal manner. The internal fragments support the surface fragments to form a flower-like structure. It can be seen from Figure 4 h that the surface of larger fragments is smoother than that of smaller fragments. Some small fragments have a layered texture on the surface, and the section is relatively flat.

Figure 4 i and Figure 4 j are microstructures enlarged by 50,000 times. Figure 4 i is the local enlargement of Figure 4 h. It can be seen from Figure 4 i that the surface of the fragment is an enlarged layered pattern with fine pores on the surface. In addition, there will be protrusions of small pieces of debris on the edge and surface of the debris. Compared with small fragments, the surface is smoother, the edge of the section is flat, and the thickness is uniform. Figure 4 k and Figure 4 l are the microstructures magnified 100,000 times. Figure 6k is the local enlarged graph of Figure 6i. From Figure 4 k, it can be further clearly observed that there are cracks on the surface of the fragments, which are not complete. And there are fragments that look like stacked layered structures. Figure 4 l is a locally enlarged graph of Figure 4 j. It can be seen from Figure 4 l that the surface of the fragment is smooth and the section is flat. There are small pieces of protuberances on the edge of the fragments. It can be measured from Figure 4 (i-l) that these nanosheets have a thickness of about 100 nm, a length of 600 nm, and a width of 200-300 nm.

By observing the surface microstructure of bismuth citrate crystals, the structural characteristics of bismuth citrate are further understood. These characteristics make it easier to form a three-dimensional network structure in gastric acid. When they are covered on the surface of the ulcer, it can achieve a better therapeutic effect on the treatment of peptic ulcer.

IV. CONCLUSIONS

In this paper, bismuth citrate was synthesized by hydrothermal method using bismuth nitrate, sodium hydroxide and citric acid as raw materials. Compared with other traditional processes, bismuth citrate synthesized by the new process has the characteristics of short time and low energy consumption.The structure was characterized by infrared, thermogravimetric, X-ray diffraction and scanning electron microscopy, and the results were analyzed. In addition, under the infrared analysis, the change of the carboxylate group of the sample bismuth citrate and the coordination mode of the carboxylate group with the metal ion Bi (III) -binary coordination mode can be understood. The relationship between sample mass and temperature can be observed in the thermogravimetric spectrum. It is calculated that the content of Bi in the final decomposition product is the same as that in bismuth citrate. It can be seen from the XRD patterns of citric acid and

International Journal of Pharmaceutical Research and Applications
Volume 8, Issue 6 Nov-Dec 2023, pp: 753-759 www.ijprajournal.com ISSN: 2249-7781

bismuth citrate that the diffraction peak of bismuth citrate at 2θ is not consistent with the diffraction peak of citric acid XRD pattern. Other peaks of citric acid did not appear in the XRD pattern of bismuth citrate, indicating that the products were not simple phase superposition. Finally, bismuth citrate was scanned by electron microscopy. The microstructure of bismuth citrate crystal was observed. From different multiples of scanning electron microscopy, from small multiples to large multiples, the samples were observed and the microstructure of the crystals was analyzed.

REFERENCES

[1]. Gong M, Zhang R, Qi JY, Wang J, Liu Q, Zhou HY, et.al. In vitro evaluation of the antibacterial effect of colloidal bismuth subcitrate on Porphyromonas gingivalis and it biofilm. Archives of oral biology, 2021,133:105300. https://doi.org/10.1016/j.archoralbio.2021.105300

[2]. Tao X , Zhang L, Du LB, Liao RY, Cai HL, Lu K, et.al. Allosteric inhibition of SARS-CoV-23CL protease by colloidal bismuth subcitrate. Chemical science, 2021,12(42):14098-14102. https://doi.org/10.1039/D1SC03526F

[3]. Abdul H Z, Zheng MY, Peng MY, Han QF.Addition of bismuth subacetate into bismuth citrate as co-precursors to improve the photocatalytic performance of Bi2O3. Materials Letters, 2019,256 : 126642. https://doi.org/10.1016/j.matlet. 2019.126642

[4]. Yoon JY, Kwak MS, Jeon JW, Cha JM. Pretreatment with Ranitidine Bismuth Citrate May Improve Success Rates of Helicobacter pylori Eradication: A Prospective, Randomized, Controlled and Open-Label Study. The Tohoku journal of experimental medicine, 2021, 255(1) : 41-48. https://doi.org/10.1620/tjem.255.41.

[5]. Guan JL, Hu YL, An P, He Q, Long H, et. al. Comparison of high-dose dual therapy with bismuth-containing quadruple therapy in Helicobacter pylori-infected treatment-naive patients: an open-label, multicenter, randomized controlled trial. Pharmacotherapy, 2022, 42 (3) : 224-232. https://doi.org/10.1002/phar.2662.

[6]. Cao Y, Zhang J, Liu Y, Zhang L,Wang L, et.al. The efficacy and safety of different bismuth agents in Helicobacter pylori first-line eradication: A multicenter, randomized, controlled clinical trial. Medicine, 2021, 100(50) : 27923. https://doi.org/10.1097/MD.0000000000027923.

[7]. Yuan S, Wang R, Chan JF, Zhang J, Cheng T, et al. Metallodrug ranitidine bismuth citrate suppresses SARS-CoV-2 replication and relieves virus-associated pneumonia in Syrian hamsters. Nature microbiology,2020,5(11)：1439-1448. https://doi.org/10.1038/s41564-020-00802-x.

[8]. Chan S, Wang R, Man K , Nicholls J, Li H, et al. A Novel Synthetic Compound, Bismuth Zinc Citrate, Could Potentially Reduce Cisplatin-Induced Toxicity Without Compromising the Anticancer Effect Through Enhanced Expression of Antioxidant Protein. Translational Oncology, 2019, 12(5)：788-799. https://doi.org/10.1016/j.tranon.2019.02.003.

[9]. Wang H. Preparation and characterization of citric acid chelated zinc, copper and manganese compounds. Hefei University of Technology, 2021. https://doi.org/10.27101/d.cnki.ghfgu.2021.001160.

[10]. Xu F, Sun X, Guo X. Analysis of main factors affecting thermogravimetric curve in thermogravimetric analysis test. Thermal Power Generation, 2005(06): 34-36+5. https://doi.org/10.19666/j.rlfd.2005.06.012.